Water Air Soil Pollut (2023) 234:178
https://doi.org/10.1007/s11270-023-06187-x

Insights into Mechanisms of Novel Engineered Biochar Derived from Neem Chips via Iron Catalyst for the Removal of Methyl Orange from Aqueous Phase

Loveciya Sunthar · Thusalini Asharp · Kannan Nadarajah

Received: 12 October 2022 / Accepted: 22 February 2023

Abstract Methyl orange (MO) is a toxic dye used in many industrial processes. The removal of MO is considered expensive by the sophisticated treatment methods. Hence, there is a need for the discovery of novel methods for removing MO from polluted water. Therefore, this study was aimed at understanding the scientific insights into the adsorption mechanism of novel engineered biochar derived from neem chips via catalytic conversion with $FeCl_3$ for the MO removal. This is the first report describing the use of novel engineered biochar derived from waste neem chip biomass for the removal of the highly resistant anionic dye "methyl orange" by understanding the insights into the removal mechanism. The biochar was prepared at different temperatures: 200 °C, 400 °C, 600 °C, and 800 °C, with a residence time of 2 h. An adsorptive experiment was planned, under a set of experimental conditions: dosage 1 g/L; pH 6; rpm 150; holding time 72 h, to identify the best biochar. The selected biochar has then been activated by iron catalyst of different concentrations (1%, 3%, 5%, and 7%) at a temperature of 700 °C for 30 min. The adsorptive performance was then checked. The engineered biochar with a high q_e value (amount of adsorbate removed by unit weight of engineered biochar) was selected, for the detailed studies; isotherm, kinetics, thermodynamics, and rate-limiting factor analyses were used to understand the adsorptive mechanism of novel engineered biochar synthesized. Moreover, it was also treated with wastewater to check its removal efficiency. Furthermore, point zero charge (pzc) was analyzed to study the functional properties of novel engineered biochar along with XRD analysis. The outcomes revealed that the $FeCl_3$ activation improved the (q_e) amount of adsorbate removed by grams of engineered biochar to 63.39 mg/g from 80.30 mg/g and it improved the aromatic carbon network. Moreover, the adsorption nature of novel engineered biochar to MO removal is multilayer. It also obeyed well for the pseudo-second-order kinetics. The adsorption is spontaneous and endothermic. The engineered biochar synthesized performed well to remove impurities from a real industrial wastewater: Removal of total suspended solids was 68% and removal of total solids was 74%. Therefore, the engineered biochar produced by the iron catalytic conversion of neem chips is a novel adsorbent for MO removal from aqueous phase.

Supplementary Information The online version contains supplementary material available at https://doi.org/10.1007/s11270-023-06187-x.

L. Sunthar · T. Asharp · K. Nadarajah (✉)
Department of Agricultural Engineering, Faculty of Agriculture, University of Jaffna, Ariviyal Nagar, Kilinochchi, Sri Lanka
e-mail: aenkanna@gmail.com

Published online: 04 March 2023

Highlights

- Novel engineered biochar from neem chips has the potential to remove industrial dyes.
- Pyrolysis temperature had a significant influence on the performance of the biochar.
- $FeCl_3$ activation of neem chips enhances the adsorption of methyl orange by two-fold.
- Surface functional properties of the biochar were improved by iron catalyst activation.

Keywords Biochar · Engineered biochar · Neem · Methyl orange · $FeCl_3$ · Wastewater treatment

1 Introduction

Water pollution by industrial dyes is considered problematic all over the world. There are many dyes which are commonly used for industrial applications (Kumar et al., 2021). However, various forms of dyes are discharged into the environment without treatment. It, in turn, causes many environmental consequences: water pollution, soil pollution, and health consequences to humans. Methyl orange is an acidic-type dye which has number of uses in textile industry, paper production, food industry, painting, and medicine (Agarwal & Vaishali, 2016). It can enter into the environment mostly by anthropogenic way, connected to the effluent from textile industries. During dying process, around 10–20% of the dyes which are used in the textile industry are released to the environment (Bazrafshan et al., 2014).

It is highly important to remove dyes from the effluent, as it can lead to some abnormal coloration to the surface water with harmful effects to aquatic organisms (Bazrafshan et al., 2014). Furthermore, it has some carcinogenic and mutagenic effects to human. The myriad treatment methods such as electrostatic, thermostatic, microbial oxidation, chemical coagulation, membrane processes, and adsorptive bubble separation methods such as foam separation (Soylu et al., 2020) and advanced oxidation processes such as Fenton oxidation process (Gökkuş et al., 2014), using ozone and ultraviolet, used for the removal of methyl orange, are highly complex and most are expensive in nature. Not only that, technical knowledge and skills are also a must to follow the advanced treatment methods. Furthermore, the complex structure and high molecular weight of the dye molecules make the removal performance through some process (microbial oxidation) insufficient (Gökkuş & Oğuz, 2011).

Therefore, there is a need for the development of simple and effective treatment methods for the removal of this toxic dye. Adsorption in this regard plays a key role in the removal of pollutants which are present in the effluent compared to the above said methods. More attention is given to low-cost absorbents for wastewater treatment. Engineered biochar is one of the low-cost absorbents, which can be used for the removal of methyl orange from the effluent. Biochar is a carbonaceous product which is produced through the pyrolysis process (Godlewska et al., 2020). When the physical, chemical, and microbial properties of biochar are changed, it is called as engineered biochar. Moreover, researchers have used various methods for the production of engineered biochar (Godlewska et al., 2020).

Iron catalyst usage is one of the chemical activation methods. The smaller pores of biochar are enriched by a smaller size of ferric cations present in $FeCl_3$ and facilitate the production of engineered biochar (Samar K. Theydan, n.d.). The studies on the use of iron catalyst for the activation of biochar from various biomass materials are at the embryonic stage. This is the first report that completely explains the mechanism of the novel engineered biochar derived from neem chip biomass using iron catalyst. The outcomes of this work are pressing to facilitate biochar research yielding highly efficient engineered adsorbents for pollutant removal from water.

Hence, this study was set towards the insights into the engineered biochar obtained from the pyrolyzed biochar obtained from neem chip activation. The systematic experimental arrangement was developed to make a comprehensive story about the novel engineered biochar from the neem chips using iron catalysts. The outcome of the study will be useful for academics, researchers, and industrial people to go for the commercialization of this effective engineered biochar efficient in the removal of the highly toxic industrial dye called "methyl orange."

2 Research Design and Methods

2.1 Materials

Neem chip was collected from Thirukkovil, Sri Lanka. A methyl orange stock solution was prepared by dissolving 1 g of methyl orange powder in 1 L of distilled water. Standard calibration curve of methyl orange is given in Fig. S.1, and Table 1 shows the chemical properties of methyl orange. All chemical reagents including iron chloride hexahydrate ($FeCl_3.6H_2O$), hydrochloric acid (HCl), sodium chloride (NaCl), and sodium hydroxide (NaOH) were of high-purity grade obtained from Organic Trading (PVT) Ltd., Sri Lanka. These were used without further purification.

2.2 Biochar Production and Characterization

The neem chips which were collected from Thirukkovil, Sri Lanka, were crushed and broken by a stone mortar and pestle. Broken shell pieces were initially sieved by 2-mm and 1-mm pore size sieves. The neem chip particles which belong to the particle size ranging from 1 to 2 mm size were collected at the end of the process. Collected particles were first washed with distilled water followed by mild acid treatment with 0.01 M HCl. Treated particles were placed for sun drying for 5 h. Heat treatment was given using a muffle furnace (Model: PC442T, Protherm Furnace, Turkey) with the heating rate of 59.52 C min^{-1} for 2 h holding time at 200 °C, 400 °C, 600 °C, and 800 °C (Al-wabel et al., 2013) temperatures by placing the particles into a ceramic crucible with a lid. Finally, obtained biochars were labeled as NCBC 200, NCBC 400, NCBC 600, and NCBC 800 respectively (NCBC: neem chip; 200: pyrolysis temperature).

The crystallographic properties of the neem chip biochar were analyzed by X_Ray Diffraction Spectroscopy (AERIS PANalytical, UK) with fixed divergent silt, cupper anode, and a long fine focus tube (40 kV and 7.5 mA) using powdered samples.

Table 1 Chemical properties of methyl orange

Chemical properties	
Chemical formula	C14H14N3NaO3S
Molar mass	327.33 g·mol^{-1}
Appearance	Orange or yellow solid
Density	1.28 g/cm^3
pH	3.1 (red) and 4.4 (yellow)
Melting point	> 300 °C (572 °F; 573 K) (not precisely defined)
Boiling point	Decomposes
Solubility in water	5 g/L (20 °C)
Solubility in diethyl ether	Insoluble

2.3 Adsorption Experiment

Batch adsorptive experiments were conducted for the neem chip biochar obtained at different pyrolysis temperatures. Each of the 25-mL flat-bottom glass bottles was filled with 20 mL of methyl orange solution with the concentration of 100 mg/L, adjusted to desired pH (pH 6) by adding 0.1 M NaOH and HCl. Each glass bottle was placed into a shaking incubator (BSD-250, Boxun, Shanghai, China) at 150 rpm and 25 °C for 72 h. Absorbance of each bottle was measured by a spectrophotometer (UH5300 Spectrophotometer, HITACHI, Japan) at 464 nm spectrum (Bazrafshan et al., 2014). Two replicates for each sample were used, and the average of the absorbance was used for further analysis. An absorbance versus biochar graph was developed using Excel version 2016. Point zero charge analysis was done by sample solutions at different ranges of pH, varying from 2 to 12, and they were placed at 150 rpm for 24 h at 25 °C. The point at which the initial pH of the solution was equal to the final pH was considered point zero charge. In other words, the net charge at this point is zero.

2.4 Biochar Activation

NCBC 600 and NCBC 800 were selected by comparing the yield and adsorptive performance. Activation was done by $FeCl_3$ at 700 °C for 20 min with different concentrations: 1%, 3%, 5%, and 7%. The impregnation ratio was maintained at 1.5:1 g/g (activator:biochar) (Samar K. Theydan, n.d.). Impregnated samples were placed into an oven at 30 °C for 24 h, and then, they were placed at 110 °C to completely dry the samples. $FeCl_3$ residues were completely removed by washing engineered biochar by 0.1 M HCl, followed by distilled water. Again the samples were placed into the oven at 110 °C for

complete drying. Adsorptive experiments were conducted again to select the best engineered biochar.

Furthermore, the effect of methyl orange concentration was investigated by changing the concentration from 100 to 500 mg/L, and the initial dosages of neem chip biochar and pH were kept 1 g/L and 6 respectively (Manoharan et al., 2022). Furthermore, the effect of pH on methyl orange removal was also studied under a set of conditions: 1 g/L initial dosage, pH ranging from 2 to 12, and 25 °C. The adsorptive capacity and removal percentage were analyzed by the following equations (Eqs. (1) and (2) respectively) (Bazrafshan et al., 2014).

$$q_e = \frac{V(C_i - C_f)}{W} \tag{1}$$

$$Removal\ percentage = \left(\frac{(C_i - C_f)}{C_i}\right) \times 100 \tag{2}$$

where

q_e amount of adsorbate removed by unit weight of absorbent in mg/g;

C_i initial concentration of adsorbate in mg/L;

C_f concentration of adsorbate at particular time in mg/L;

W weight of biochar in grams; and

V volume of solution in liters.

2.5 Isotherm, Kinetics, Thermodynamics, and Rate-Limiting Factor Analyses

Adsorption isotherm, kinetics, thermodynamics, and rate-limiting factor analyses were performed to understand the mechanism of MO adsorption by the novel engineered biochar, using mathematical models. The Freundlich model, Langmuir model, and Temkin model were used for the analysis of the adsorption isotherm. The nature of adsorption was identified through the isotherm study. The kinetics study was done by the pseudo-first-order equation, pseudo-second-order equation, Elovich, and Avrami models. The Van't Hoff equation was used for thermodynamics, and the rate-limiting factor was studied by the Weber-Morris model. The respective equations starting from 1 to 10 are given in Supplementary Data.

2.6 Wastewater Treatment

An artificially polluted wastewater sample was treated with 7% NCBC 800 engineered biochar. Adsorptive experiment was conducted and changes in some selected parameters (DO, EC, color, turbidity, pH, TS, TDS, and TSS) were measured before and after adsorption to compare the efficiency of the engineered biochar for wastewater treatment. Figure 1 represents the overall experimental steps used to systematically study the set objectives. This engineered biochar from neem chips was developed via two steps as indicated in Fig. 1, the detailed and complete procedures used to understand the adsorptive mechanism of novel engineered biochar.

3 Results and Discussion

3.1 Biochar Characterization

3.1.1 Effect of Temperature

A reduction in the yield of the neem chip biochar was observed. The yield of the neem chip biochar reduced with increasing temperature. The yield of the neem chip biochar reduced from 91.2 to 8.3% as pyrolysis temperature changed from 200 to 800 °C. The average yields of NCBC 200, NCBC 400, NCBC 600, and NCBC 800 were 91.2%, 31.5%, 14.3%, and 8.3%, respectively, as shown in Fig. 2. The highest yield, 91.2%, at pyrolysis temperature 200 °C was due to partial pyrolysis of neem chip biomass (Manoharan et al., 2022). Pyrolysis temperature, heating rate, and holding time are the limiting factors on the yield of biochar. Here, the heating rate (59.52 °C) and holding time (2 h) were constant, and pyrolysis temperature was the limiting factor for biochar yield.

The yield reduction is for the sake of combustion of primary and secondary components. Thermal decomposition of lignin and some other materials leads to the production of biochar. During heat treatment, destruction of cellulose, hemicellulose, and some organic components occurs with increasing pyrolysis temperature (Al-wabel et al., 2013).

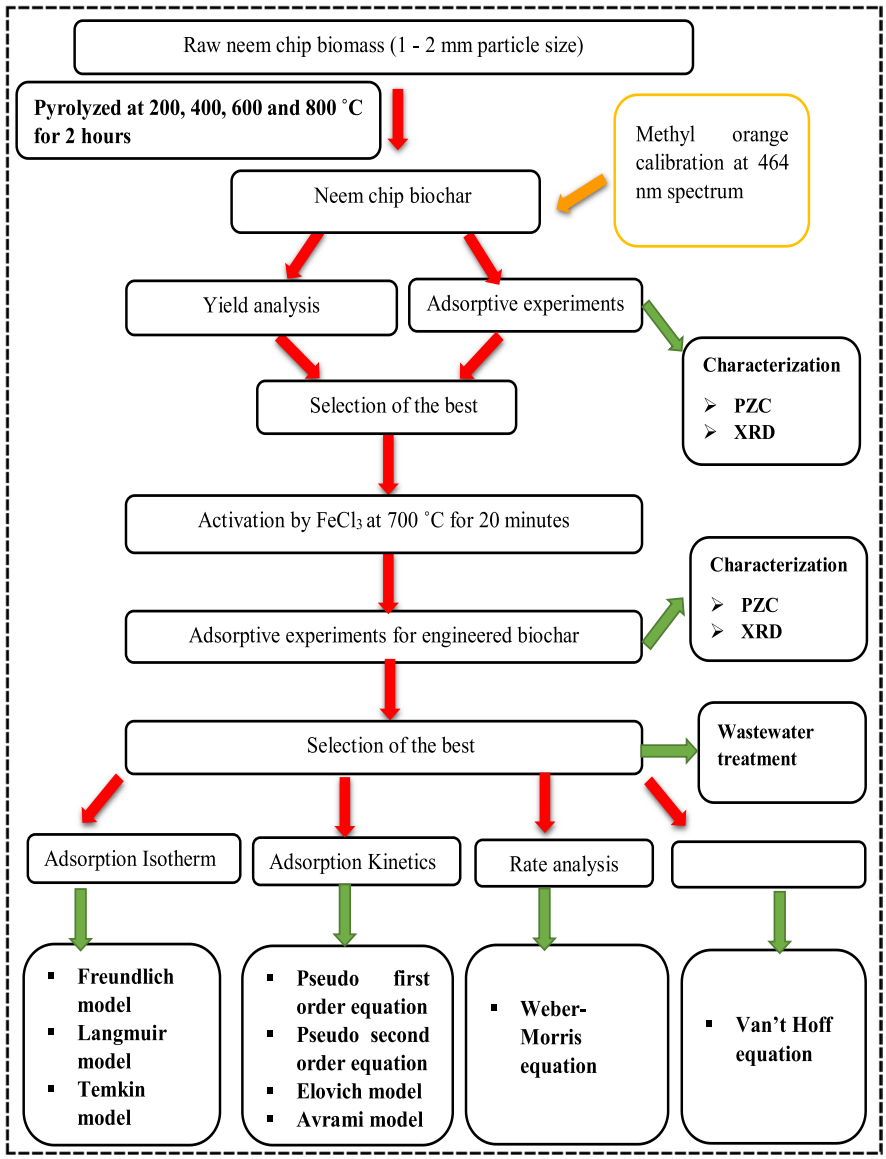

Fig. 1 Overall display of experimental setup

Due to the thermal effect for certain time duration, the volatile materials are lost as vapor form, and a portion of the solid material is converted into ash (Bonelli et al., 2001). Therefore, a yield reduction was observed with an increasing rate of volatilization with increasing pyrolysis temperature. In contrast, the ash content of the biochar was increased with increasing pyrolysis temperature. Similar pattern in yield was observed in previous studies (Al-wabel et al., 2013), and the reduction in yield was changed from 51.3 to 23.1% as pyrolysis temperature was changed from 200 to 800 °C.

The pyrolysis process increases the carbonization of biomass material (Al-wabel et al., 2013). An increase in reduction of yield and increase in porosity were observed with increasing pyrolysis temperature. Clogging of pores on the biochar surface occurred in lower pyrolysis temperatures (Kloss et al., 2012). It matches with earlier reported works by Al-wabel et al. (2013) and Manoharan et al. (2022), and the reduction of yield was 51.3 to 23.1% and 46.8 to 5.1% respectively for the pyrolysis temperatures ranging from 200 to 800 °C and 300 to 900 °C.

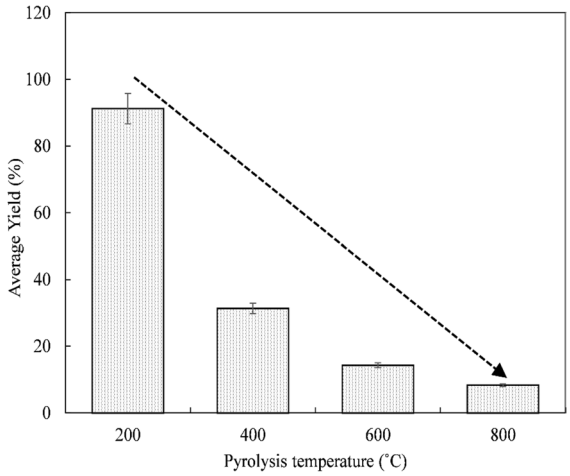

Fig. 2 Effect of pyrolysis temperature on biochar yield

3.1.2 Surface Charge Distribution

The presence of positive and negative charges at point zero charge (pzc) point is equal, and the net charge is zero. There was an increase in the pzc of the biochar pyrolyzed at different temperatures: 200 °C, 400 °C, 600 °C, and 800 °C. The pzc for NCBC 200, NCBC 400, NCBC 600, and NCBC 800 were 4.9, 5.1, 7, and 8.9, respectively, as shown in Fig. 3. It is obvious that the stabilized aqueous solution will be positively charged when the pH of the solution is below the identified pzc, and it is vice versa for highest pH values (Nadarajah et al., 2021). As the experimental setup was prepared by NaOH, NaCl, and HCl, negatively charged sites were computed by Na^+ and H^+ ions, and positively charged sites were computed by OH^- and Cl^- ions (Manoharan et al., 2022).

The best and optimum pH for methyl orange adsorption can be determined by pzc analysis (Farooq & Ramli, 2011). If the pzc is less than the pH of the solution, then the surface of the biochar is negative. It leads to the adsorption of positively charged ions. This story is reverse as the pH goes the other way around. The charge distribution of biochar is highly essential for the adsorption. The structure of the biochar should be kept positive, if anionic dyes need to be adsorbed. However, it has to be negative if cationic dyes are used for adsorption (Manoharan et al., 2022). As methyl orange is considered an anionic azo dye (Bazrafshan et al., 2014), the structure of the biochar should be positive for the better removal. Therefore,

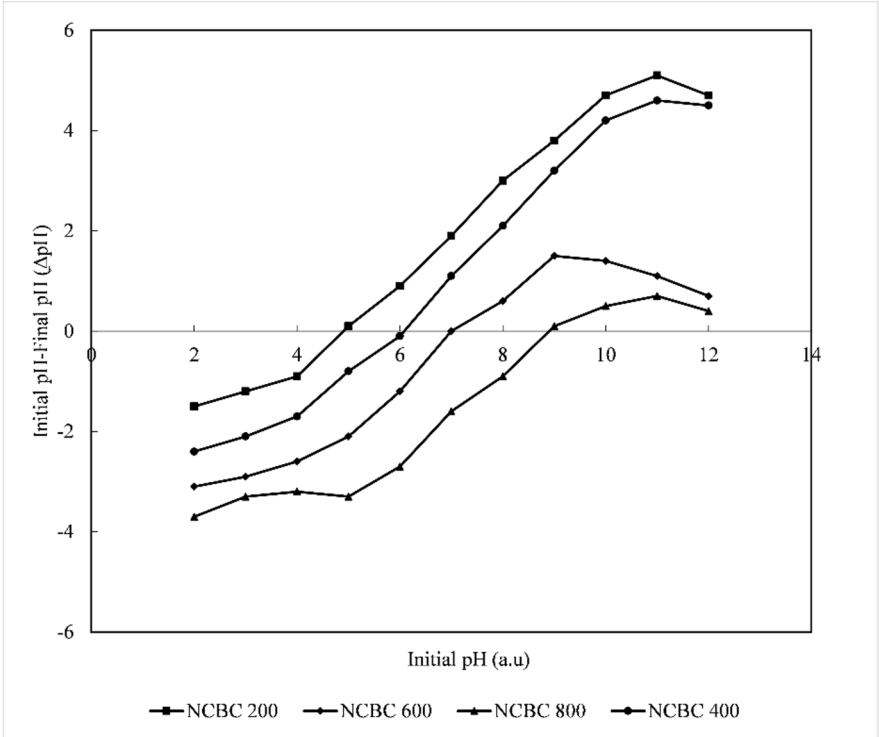

Fig. 3 Point zero charge analysis of biochar pyrolyzed at different temperatures

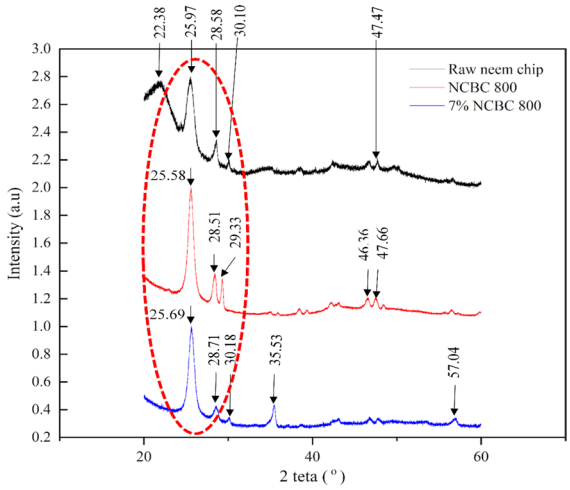

Fig. 4 XRD spectra of the raw neem chip, biochar NCBC 800, and engineered biochar 7% NCBC 800

the pH of the adsorptive medium should be less than the pzc of the biochar (Farooq & Ramli, 2011).

3.1.3 Carbon Structure

The crystalline properties of the materials were analyzed by XRD spectrum. XRD spectra of the raw neem chip, neem chip biochar pyrolyzed at 800 °C (NCBC 800), and engineered biochar derived from neem chips (7% NCBC 800) are illustrated in Fig. 4. The spectra in Fig. 4 show several peaks corresponding to above said biomass materials derived from neem chips. The strong peak was observed at a 2θ value of 25.59° for the raw neem chip and NCBC 800, and it was 25.62° for 7% NCBC 800. It was continued by 2θ values of 28.62°, 28.41°, and 28.60° for the raw neem chip, NCBC 800, and 7% NCBC 800 respectively. Compared to the raw neem chip and NCBC 800, a strong peak was observed for 7% NCBC 800 at a 2θ value of 35.53°. Superficial peaks were observed at the posterior part of the XRD spectrum, where 2θ values for the raw neem chip, NCBC 800, and 7% NCBC 800 were 46.38°, 46.36°, and 46.52° respectively.

As comparison, the sharpness and intensity of peak increase from the raw neem chip to NCBC 800 and 7% NCBC 800. This proves the crystallization of carbon (Song et al., 2013). The formation of the strongest peaks is a good evidence for the development of crystals (Silicates) and inorganic compounds ($CaCO_3$) during heat treatment (Manoharan et al., 2022). A very fine crystal structure is explained by the larger peak width of the XRD spectrum (Zhu et al., 2000). Furthermore, a wide peak was observed at the beginning of the spectrum for the raw neem chip compared to NCBC 800 and 7% NCBC 800. Apparently, a peak was observed at a 2θ value of 35.53° on the spectrum of 7% NCBC 800. It represents the effect of ferric chloride catalyst on biochar structure with carbon network developed.

The peak at 2θ values at 28° is due to the presence of silicates (Berwal et al., 2015). This is in line with earlier study using lignocellulosic biomass and biochars, where the peak was observed at 28.4° (Berwal et al., 2015). Silicates are one of the structural components of bark. The intensity of diffraction peaks relies on the amount of substances present in the powdered sample.

3.2 Adsorptive Experiment

Different adsorptive phenomena will lead to the formation of different size pores in the biochar surface (Bonelli et al., 2001). In addition to above, the raw

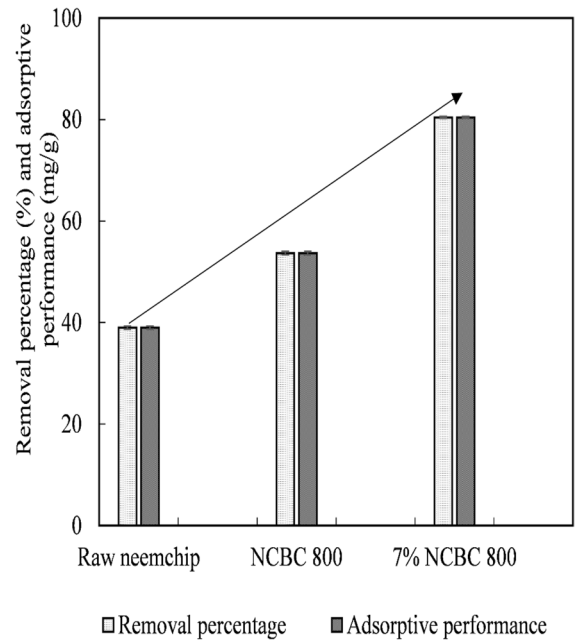

Fig. 5 Removal percentage and adsorptive performance (q_e) of raw, neem chip biochar, and engineered biochar

neem chip, neem chip biochar, and engineered biochar derived from the neem chip were also compared to check the effectiveness of the engineered biochar on adsorptive performance and removal percentage of methyl orange. The results obtained after adsorptive experiment are shown in Fig. 5. As shown, the adsorptive performance of the engineered biochar (7% NCBC 800) was higher than that of the neem chip biochar and raw neem chip. The heat treatment through pyrolysis process increased the adsorptive performance on both the neem chip biochar and engineered biochar. Moreover, the adsorptive performance of the engineered biochar is enhanced by the addition of $FeCl_3$ (Nadarajah et al., 2021). In addition to surface functional groups, the microstructure of biomass also improved by the catalytic effect of $FeCl_3$ (Sajjadi et al., 2019). This is in agreement with the results of earlier studies using $FeCl_3$ as a catalytic agent to remove contaminant particles from water (Nadarajah et al., 2021).

Different structural components associated with biomass material show different thermal reactions with respect to pyrolysis temperature. Moreover, the mineral materials on the biomass surface can show a catalytic effect on biochar production. Furthermore, iron catalyst also enhances the properties of surface functional groups (Bonelli et al., 2001). Therefore, an increase in adsorptive performance was observed in engineered biochar from neem chips compared to the biochar. As pyrolysis temperature increased, basic functional groups and highly ordered aromatic groups were also increased (Al-wabel et al., 2013). It leads to the adsorption of dye particles from aqueous solution. Similar results were recorded on the studies related to biochar produced from *Conocarpus* waste and study on thermal degradation rates of Brazil nut shells (Bonelli et al., 2001).

The effect of the raw neem chip, biochar NCBC 800, and engineered biochar 7% NCBC 800 on methyl orange removal is shown in the Supplementary Information by Plate S.1., where Plate S.1(a) indicates the experimental setup before adsorption. Similarly, the observations after adsorption are shown in Plate S.1(b). The reduction of color of the aqueous solution is a good evidence to understand the effectiveness of 7% NCBC 800 than the other two. Adsorptive performances of different materials activated by various technologies were compared, and the results are tabulated in Table 2. A significance in adsorptive performance ($q_e = 80.3$ mg/g) was obtained for engineered biochar derived from neem chips. Therefore, the research result reported in this paper is an effective solution for dye removal from aqueous phase.

3.3 Factors Influencing Methyl Orange Removal

3.3.1 Dosage of Activated Carbon

The effect of engineered biochar dosage was studied at 25 °C with 100 mg/L concentration of methyl orange solution (pH 6). Engineered biochar dosage ranged from 0.5 to 5 g/L. Figure 6 explains the adsorptive performance of 7% NCBC 800 with different dosages (0.5, 1, 2, and 5 g/L). It was noticed that the increasing dosage considerably enhanced the adsorptive performance. However, the removal percentage increased at a decreasing manner from 37.02 to 97.40% for the changes in the dosages from 0.5 to 5 g/L as the availability of methyl orange particles is limited in each solution. Availability of adsorbent surface is high with respect to increasing dosage (Farooq & Ramli, 2011). Therefore, higher removal performance was observed for higher dosages, and for lower dosages, it was vice versa.

The adsorption process mainly depends on the surface properties. Available surface area and mass of adsorbent can affect the adsorption efficiency (Bazrafshan et al., 2014). The greater amount of active sites for adsorption leads to the increase of adsorptive performance. The influence of iron catalyst plays an important role in the enhancement of adsorptive performance. During the activation process, larger particles in the biochar were broken down into many small-sized particles (Nguyen et al., 2021) by the effect of iron catalyst. It induces the number of active sites and adsorptive performance as well. The porous structure of the engineered biochar facilitates the removal of the methyl orange dye (Lonappan et al., 2018).

Moreover, the surface functional groups which are activated by iron catalyst lead to the internal adsorption of dye particles. Throughout the experiment, a reduction in adsorptive performance q_e (mg/g) was observed with increasing dosage. The q_e values for dosages 0.5, 1, 2, 3, and 5 mg/L are 74.05, 64.09, 42.46, 30.61, and 19.48 mg/g respectively. The amount of methyl orange removed by unit weight of the engineered biochar is reduced with increasing dosage (Hamzezadeh et al., 2022). A previous study related to treating cationic dye

Table 2 Adsorptive performance of different materials for methyl orange removal

Material used	Dosage (mg/L)	pH (a.u)	Temperature (˚C)	q_e (mg/g)	References
Vitis viticola. L grape activated by calcination process	1 g/L	2	45 ˚C	79.9	(Yonten et al., 2020)
Coconut shell activated by furnace induced activation and $ZnCl_2$ chemical activation	1 g/L	Natural pH	30 ˚C	59.17	(Hii, 2021)
Mandarin peels activated by NH4Cl (MN-Biochar) and ZnCl2 (MZ-Biochar)	1.5 g/L	7	25 ˚C	MN-Biochar: 2.52 MZ-Biochar: 16.27	(Park et al., 2021)
Engineered biochar derived from neem chips using FeCl3	1 g/L	6	25 ˚C	80.30	Reported work in this paper

also reported similar pattern (Hamzezadeh et al., 2022), where removal performance was reduced from 34.2 to 6.74 mg/g for an increasing dosage of 0.5 to 4 g/L.

3.3.2 pH

The pH of the solution plays an important role in the adsorptive removal of the dye as it has the influence on surface charge, functional properties of active sites, structure of adsorptive material, and degree of ionization of adsorbate material (Bazrafshan et al., 2014). The effect of initial pH on methyl orange removal was studied at different pH levels ranging from 3 to 11 at 25 °C with 1 g/L dosage and 100 mg/L initial concentration of the methyl orange solution. The initial pH of the solution is one of the factors

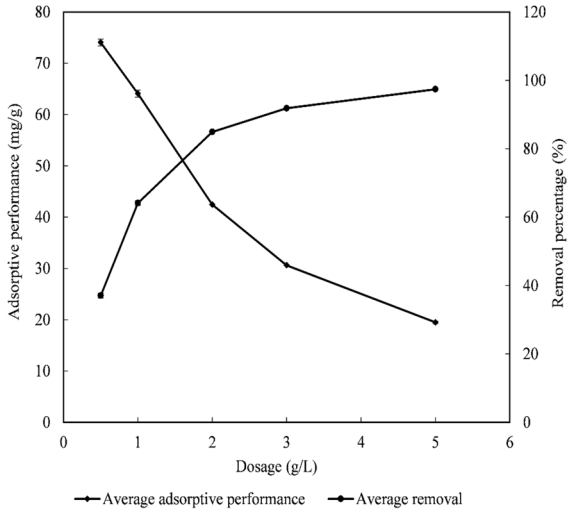

Fig. 6 Effect of dosage on methyl orange removal by engineered biochar

which influences the methyl orange removal performance by any biochar as it has the influence on the surface structural, functional groups, and net charge (Pal et al., 2013). The effect of initial pH on methyl orange removal is illustrated by Fig. 7. The amount of the dye removed by unit weight of the engineered biochar was high (81.55 mg/g) for acidic pH (pH 4), and low (61.02 mg/g) for pH 11. A reduction by a fluctuating manner in adsorptive performance was observed for basic pH values. It was observed that the pzc value for 7% NCBC 800 was 4.16 based on Fig. S.2 in the Supplementary Information. It indicates that the values below this value can lead to the surface of engineered biochar positively charged.

Methyl orange is anionic azo dye (Block et al., 2021), adsorptive performance is high at lower and acidic pH values, and it is reduced with increasing negative charges. As the initial pH values of the aqueous solution exceed the pzc, the net charge of the engineered biochar remains negative, and an impulsive effect can be observed between the adsorbate and adsorbent. A study by Zhang et al., (2011) on Congo Red adsorption by ball-milled sugarcane bagasse also reported similar pattern.

3.3.3 Initial Concentration

The effect of the initial concentration on adsorptive performance (q_e) of the engineered biochar for methyl orange removal at 25 °C is illustrated by Fig. 8. A reduction in the removal performance was observed with increasing initial concentrations (He et al., 2014). The highest removal percentage (96.19%) was observed at the 50 mg/L initial concentration with an adsorptive performance of 48.09 mg/g. Removal performances were 96.19%, 80.3%, 73.72%, 80.03%, and 64.14% for 50 mg/L, 100 mg/L, 150 mg/L, 200 mg/L, and 300 mg/L of concentrations respectively. This is noteworthy as equal dosage (1g/L) of engineered biochar has been used for all experimental arrangements, and adsorptive performance is limited by the availability of active sites (Pal et al., 2013).

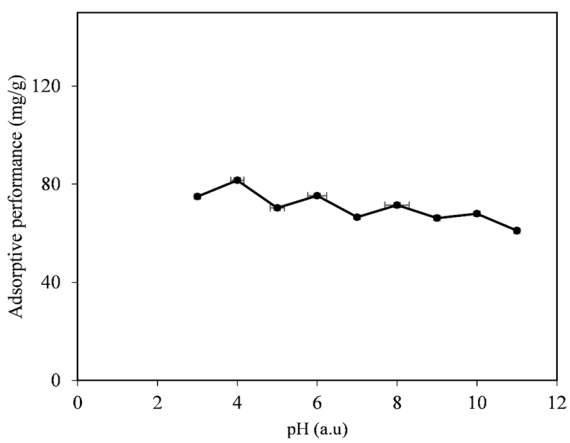

Fig. 7 Effect of initial pH on methyl orange removal (temperature 25 °C; dosage 1 mg/g; initial concentration 100 mg/L)

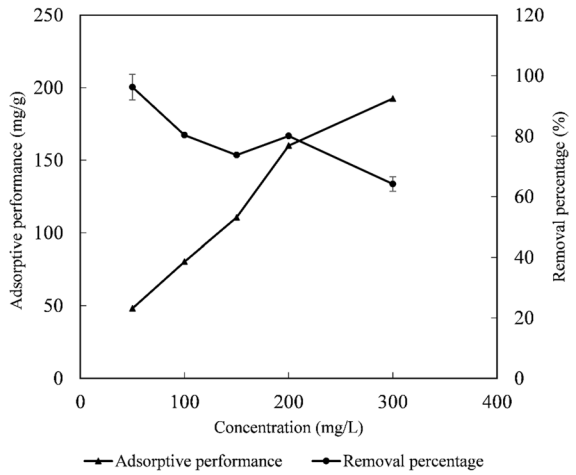

Fig. 8 Effect of initial concentration on methyl orange removal by engineered biochar (pH 6; temperature 25 °C)

The fact is that the higher mass of adsorbent availability can expedite the attractive forces among adsorbent and adsorbate surfaces (Nadarajah et al., 2021). The ratio between active sites and methyl orange particles is high for lower concentrations. Therefore, high removal percentage was observed (Garg et al., 2003). It is conflicting for higher concentrations (Hamzezadeh et al., 2022). A hypsochromic shift was observed for lower initial concentrations of methyl orange than higher concentrations. This observation is due to the availability of high number of pollutant particles in the aqueous solution with limited number of adsorptive sites. A similar pattern was proved by a study on "Adsorptive removal of methyl orange and reactive red 198 dyes by *Moringa peregrina* ash" (Bazrafshan et al., 2014). A decrease in the removal performance from 97.6 to 80.21% and an increase in q_e from 1.39 to 17.19 mg/g for methyl orange were observed in the above reported work.

3.4 Isotherm Model Outcomes of the Engineered Biochar

Sorption mechanism, surface properties of adsorbent, and adsorbate interaction can be explained through adsorption isotherms (Mohammadi et al., 2011). The well-known and common isotherm models: the Langmuir isotherm model, Freundlich isotherm model, and Temkin isotherm model, were used to investigate the effect of adsorption by (engineered biochar from neem chip by 7% FeCl3) 7% NCBC 800 on methyl orange removal. The linear forms of each model: Langmuir, Freundlich, and Temkin models (explained in Eqs. 1, 2, and 3 respectively in the Supplementary Information), were used for the mathematical analysis. Figure 9

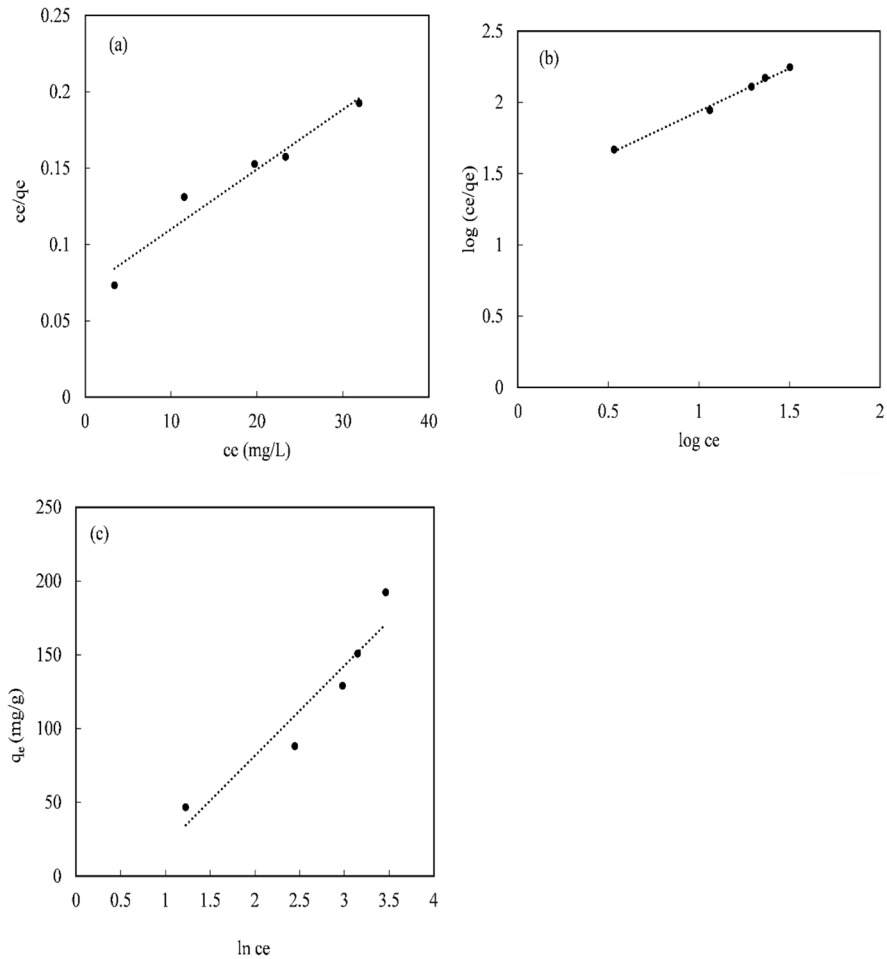

Fig. 9 Isotherm analysis of engineered biochar for methyl orange adsorption: Langmuir (**a**); Freundlich (**b**); Temkin (**c**) (pH 6, temperature 25 °C, concentration 100 mg/L, and dosage 1 g/L)

explains the results of the isotherm analysis of methyl orange adsorption by the engineered biochar derived from neem chips (where (a) is the outcome of the Langmuir isotherm model; (b) outcome of the Freundlich isotherm model; and (c) outcome of the Temkin isotherm model). The obtained values of Langmuir constant (K), coefficient of heterogeneity (n), Temkin isotherm constant (At), constant related to heat adsorption rate (Bt), and regression value (R^2) for the respective models are tabulated in Table 3.

Among the three isotherm models used, the adsorption process of methyl orange was well-fixed with the Freundlich isotherm model with the highest R^2 value. The obtained R^2 values were 0.9482, 0.994, and 0.9056 for Langmuir, Freundlich, and Temkin models respectively. Better fix of the Langmuir model explained that the methyl orange particles were presumed to have been adsorbed as a monolayer by active sites of engineered biochar from neem chip (Bazrafshan et al., 2014). At the same time, adsorption process through heterogeneous surfaces can be explained by the Freundlich model, and Temkin isotherm model explained the linear reduction of the adsorption heat (Manoharan et al., 2022). The highest overall regression value (R^2) of 0.994 and coefficient of heterogeneity ($1/n$) of 0.6 indicate that a heterogeneous adsorption process also occurred with multilayers of absorbent. Previous adsorption studies reported that the fall of heterogeneity between 0 and 1 was an indication of favorable adsorption process (Manoharan et al., 2022), and it was reported as 0.544 for that study using neem chip biochar.

3.5 Adsorption Kinetics

The kinetics study was conducted for 3500 min to determine the controlling mechanism of 7% NCBC 800 on methyl orange removal. The linear forms of the pseudo-first-order, pseudo-second-order, Elovich, and Avrami models were used to study the kinetic parameters. Figure 10 indicates the kinetic study of 7% NCBC 800 for methyl orange removal by the pseudo-first-order (a), pseudo-second-order (b), Elovich (c), and Avrami (d) models.

The corresponding parameters: K_1—adsorption rate constant of the pseudo-first-order model, K_2—adsorption rate constant of the pseudo-second-order model, α—initial adsorption rate and β—desorption constant (Soldatkina & Zavrichko, 2019), and expected (q_e.Exp) and calculated (q_e.Cal) values of adsorptive performance, 570 obtained from the linear graphs, are summarized in Table 4.

The R^2 values obtained for 50 mg/L, 100 mg/L, and 150 mg/L concentrations were 0.9601, 0.9319, and 0.7186 respectively for the pseudo-second-order model. Based on the results, the pseudo-second-order model is well fixed with the adsorption, compared to the pseudo-first-order, Elovich, and Avrami models. Dye uptake rate can be explained by the adsorption kinetics with control of time (Soldatkina & Zavrichko, 2019) at solid–liquid interface. The pseudo-second-order model explains that the adsorption is controlled by chemical reactions (Godlewska et al., 2020) between the adsorbent surfaces. Similar results were reported in already published research studies (Ahmed Jasim & Mohammed Abbas, 2019; Godlewska et al., 2020; Wasewar et al., 2009). The recorded R^2 values were ranging from 0.994 to 1.000 for the above studies.

The pseudo-second-order model eliminates the influence of equilibrium concentration. It gives better understanding of adsorption mechanism. As the adsorption of methyl orange is through chemisorption process, relatively longer time is required to reach equilibrium. Furthermore, it generates poor fit for the kinetic analysis (Nadarajah et al., 2021). At this point, it is worthwhile to note that the effect of contact time on dye adsorption at different initial concentrations is explained by kinetic models (Samar K. Theydan, n.d.). The above results are in conformity with reported works in past researches on "Adsorption of methylene blue onto biomass-based activated carbon by $FeCl_3$ activation" (Samar K. Theydan, n.d.). With 4.5 h of holding time, 235.55 mg/g of q_e was recorded in the above said study.

Table 3 Isotherm parameters for methyl orange removal by 7% NCBC 800

Dye	Langmuir			Freundlich			Temkin		
	q_m	K_1	R^2	$1/n$	K_f	R^2	A_t	B_t	R^2
Methyl orange	256.41	0.06	0.95	0.60	21.65	0.99	0.41	40.67	0.91

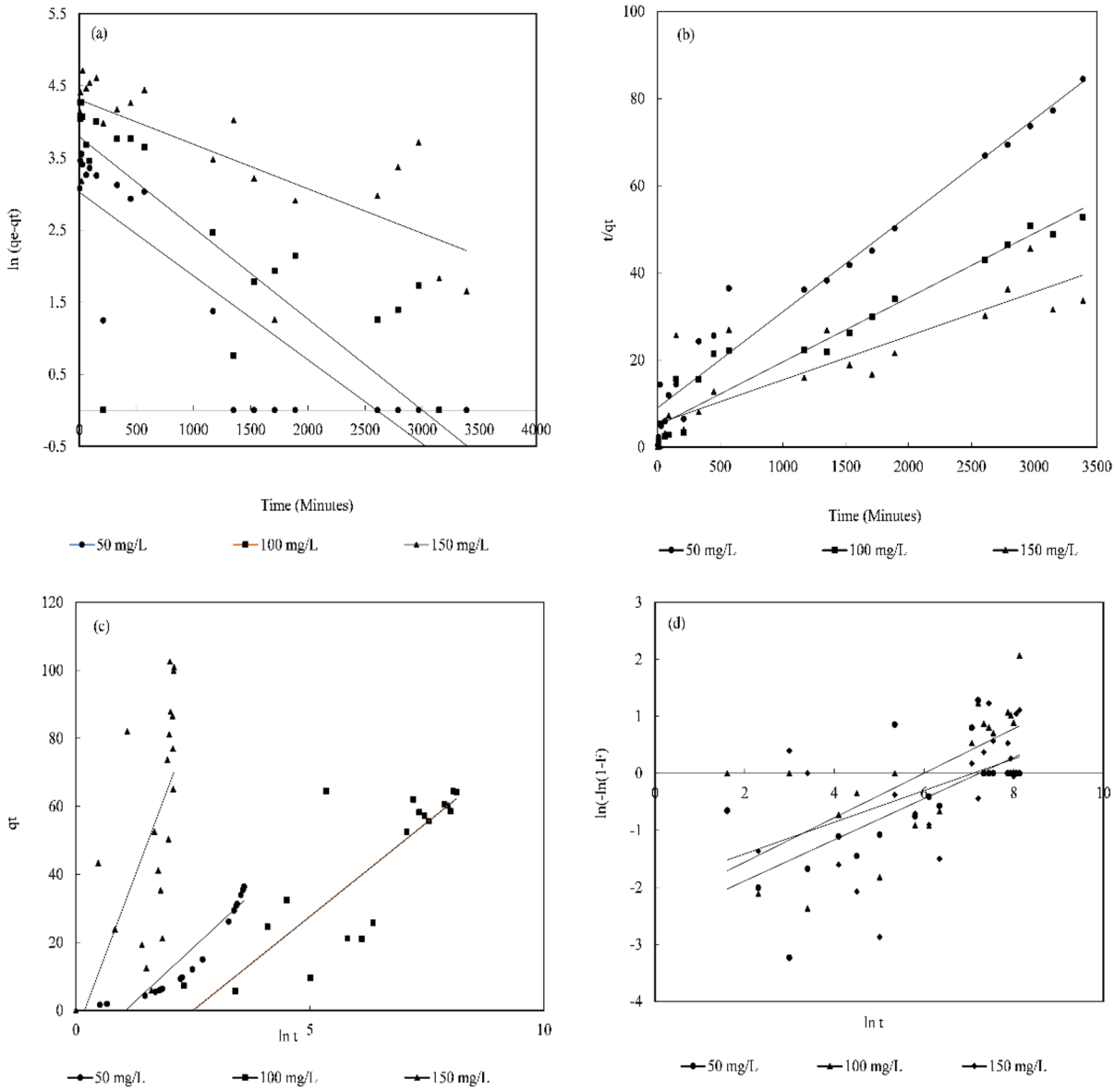

Fig. 10 Different kinetic models for methyl orange adsorption by engineered biochar: pseudo-first-order model (**a**); pseudo-second-order model (**b**); Elovich model (**c**); Avrami model (**d**)

3.6 Adsorption Thermodynamics

A thermodynamic study is essential to ensure the independence of adsorption process (Bazrafshan et al., 2014). Gibbs free energy change ($\Delta G°$) is the major indicator for spontaneity (Mohammadi et al., 2011). The voluntary nature of adsorption reaction is indicated by the negative value for $\Delta G°$. The rate equation and the Van't Hoff equation mentioned in Eqs. 2.10 and 2.11, respectively, were used to study the thermodynamic parameters: Gibb's free energy change ($\Delta G°$), change in enthalpy ($\Delta H°$), and change in entropy ($\Delta S°$). Among these thermodynamic parameters, change in enthalpy ($\Delta H°$) and change in entropy ($\Delta S°$) were directly obtained from the slope and intercept of log Kd versus 1/T curve as shown in Fig. 11. Gibb's free energy can be determined by enthalpy and entropy factors.

Table 4 Different kinetic parameters obtained for methyl orange removal by 7% NCBC engineered biochar

C_i (mg/L)	Pseudo-first-order				Pseudo-second-order				Elovich			Avrami	
	q_eCal. (mg/g)	q_eExp. (mg/g)	K_1	R^2	q_eCal. (mg/g)	q_eExp. (mg/g)	K_2	R^2	α	β	R^2	n	k
50	20.58	36.32	0.0012	0.7756	45.2488	36.32	0.00005	0.9601	36.56198	0.0786473	0.8995	0.3607	13.588
100	44.35	64.21	0.0012	0.5948	68.027	64.21	0.00004	0.9319	134.6756	0.0904486	0.7829	0.3898	10.3563
150	74.11	106.07	0.0007	0.5439	99.009	106.07	0.00001	0.7186	44.2235	0.0253357	0.2843	0.2772	7.144

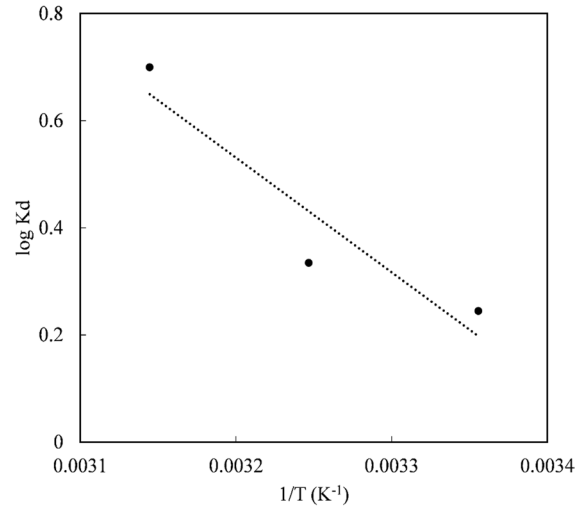

Fig. 11 Relationship between log Kd and 1/T

Table 5 Thermodynamic parameters of methyl orange removal by 7% NCBC 800

Dye	Temperature (K)	Thermodynamic parameters		
		$\Delta G°$ (kJ/mol)	$\Delta H°$ (kJ/mol)	$\Delta S°$ (kJ/mol/K)
Methyl orange	298	− 1.048	40.97	0.141
	308	− 2.458		
	318	− 3.868		

Moreover, Table 5 explains the thermodynamic parameters of methyl orange adsorption by engineered biochar. The $\Delta G°$ values were − 1.048, − 2.458, and − 3.868 kJ/mol for 25 °C, 35 °C, and 45 °C respectively. This observation indicates that the adsorption of methyl orange by the neem chip engineered biochar is spontaneous. Furthermore, previous studies related to adsorptive removal of methyl orange also reported similar results (Mohammadi et al., 2011): − 25.85, − 25.94, and 26.26 kJ/mol respectively for the temperatures of 25 °C, 40 °C, and 60 °C. The positive value (40.97 kJ/mol) of $\Delta H°$ indicates that the process of methyl orange removal is endothermic. This is due to higher intake of heat energy than the release into the system. In addition, the change in entropy ($\Delta S°$) was also a positive value, and it is 0.141 kJ/mol/K.

3.7 Rate-Limiting Analysis of Methyl Orange Removal by 7% NCBC 800

The data obtained from the kinetics study was used for the rate-limiting factor analysis. The movement of particles onto the surface and into the pores of the adsorbent can be well explained by the rate-limiting analysis. Furthermore, the rate-limiting process during adsorption can also be understood by this analysis. Investigation of the rate-limiting factor was done by the well-known Weber-Morris model. Figure 12a illustrates the linear plot of qt vs $\sqrt{t}$. The kwm (inter particle diffusion rate) and I (thickness of boundary layer) were obtained from slope and intercept, respectively, for three different concentrations. The relationship between kwm/I and initial concentration is shown in Fig. 12b.

Two distinct phases for methyl orange adsorption are revealed by the Weber-Morris model. Phase I (first linear component) of the qt vs $\sqrt{t}$ plot reflects mass movement of methyl orange from the solution to the boundary layer of the biochar, while phase II (second linear portion) represents the intra-particular diffusion as well as the effect of the boundary layer (Campos et al., 2018). Very slow rate of increase was observed in the 50 mg/L concentration. A bit speed was observed for 150 mg/L, and the rate was moderately higher for the 100 mg/L concentration of the methyl orange solution. It is because of the movement of methyl orange particles towards the surface of engineered biochar.

Moreover, the availability of high number of adoptive sites induces the rate of external mass transfer at the beginning of the adsorption (Manoharan et al., 2022). However, a reduction in active sites with time leads to the decreasing tendency of graph at phase II. Similar pattern has been reported in previous studies on the removal of methyl orange by different types of biochar materials (Bazrafshan et al., 2014). Adsorption process is controlled by more than one factor, especially by multilayer and intra-particular diffusions and also with time. The influence of every factor causes the reduction in adsorptive performance (Bhattacharyya & Sharma, 2005).

3.8 XRD Spectra

Figure S.3 represents the XRD spectra before and after the adsorption of methyl orange by the engineered biochar derived from neem chips via iron catalyst (7% NCBC 800). Similar pattern of XRD spectra was observed for before and after adsorption of methyl orange. Remarkable peaks at 2θ values of 25.97°, 28.84°, 35.78°, 43.48°, and 57.13° and a barely visible peak at a 2θ value of 35.15° were obtained for 7% NCBC 800 as shown in Fig. S.3 in the Supplementary Data. The intensity of the strong peak (2θ value of 25.97°) in respective spectra obtained for after adsorption is getting increased from 0.71 to 0.98 due to the adsorption of methyl orange by 7% NCBC 800. Comparison of the spectrum obtained before adsorption and the spectrum obtained after adsorption revealed some weak peaks (2θ value of 47.1) and humps (2θ value of 48.44) along the spectrum obtained after the adsorption of methyl orange. The changes in pattern of the spectra responsible to study the adsorption behavior of the engineered biochar for methyl orange are a good evidence to confirm that the dye molecules diffused

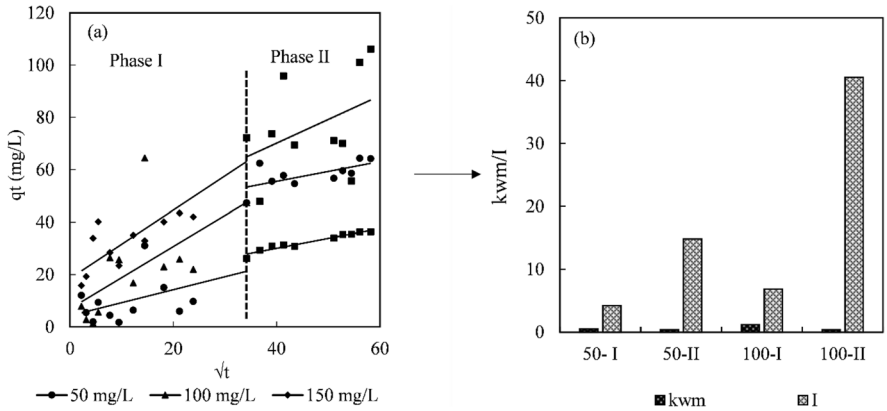

Fig. 12 Outcomes of the rate-limiting analysis for methyl orange removal by 7% NCBC 800

into micro- and macro-pores of engineered biochar derived from neem chips (Namasivayam & Kavitha, 2006).

3.9 Outcomes for Wastewater Treatment

Figure 13 represents the different measured parameters of polluted wastewater with dye addition, before and after the adsorptive experiment. The effectiveness of 7% NCBC 800 (engineered biochar from neem chip biochar by 7% $FeCl_3$) on artificially polluted wastewater was analyzed. Changes in DO, EC, pH, color, turbidity, TS, TDS, and TSS were plotted for polluted wastewater before and after adsorption. Significant changes were observed in DO, EC, pH, color, TS, and TSS. However, turbidity and TDS were not showing a significant change. A gradual decrease was observed in DO before and after the adsorption of polluted wastewater.

A drastic reduction in color was observed before and after adsorption. Color value was reduced from 456 to 11.48 after adsorption by 7% NCBC 800. The highest value was observed for color initially due to the addition of the methyl orange dye. The reduction of color is due to the adsorptive removal of dye particles as well as some other solid particles which are present in artificially polluted wastewater sample.

A reduction in turbidity is also an evidence for the occurrence of adsorption by engineered biochar derived from neem chip. Like other parameters, solid contents of the artificially polluted wastewater sample were reduced because of the adsorption process. From all of the observations of wastewater treatment, the 7% NCBC 800 can be used for the wastewater treatment. Above way, similar type of adsorptive removal

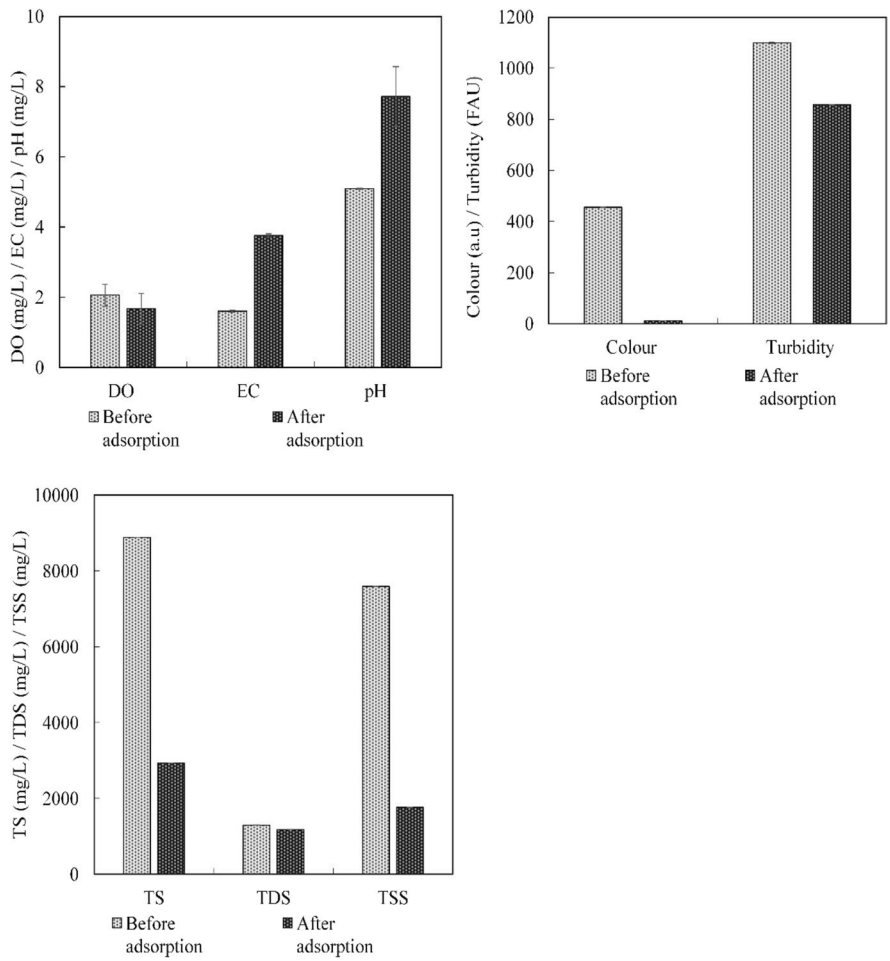

Fig. 13 Measured parameters of polluted wastewater samples treated with engineered biochar: DO, EC, and pH changes (**a**); color and turbidity changes (**b**); TS, TDS, and TSS changes (**c**)

mechanism has been observed in several other studies targeting wastewater treatments with different kinds of biochar materials (Kumar et al., 2021).

Engineered biochar, in this study, is a carbon-rich material, produced with limited oxygen by heating the biomass at high temperatures through a pyrolysis process and treated with catalyst before activation. As a result of its high porosity, enhanced surface area, high cation, and anion exchange capacity, biochar is able to hinder contaminants and pollutants from wastewater (Chai et al., 2021). Furthermore, it reduces the bioavailability of pollutants by adsorption (Chai et al., 2021). This is why the engineered biochar is used in wastewater treatment. It also gave good outcome for the wastewater treatment.

4 Conclusions

The study mainly focused on the performance of engineered biochar via $FeCl_3$ catalytic activation from the neem chip biochar for the removal of the methyl orange dye from aquatic phases effectively. The pyrolysis temperature had a significant effect on the functional properties of biochar. The biochar NCBC 800 has the highest q_e value of 63.39 mg/g for methyl orange. The novel $FeCl_3$ catalyst induced the performance of engineered biochar significantly, and it yielded the adsorptive performance of 80.30 mg/g (Langmuir maximum value was 0.95). The adsorptive performance of 7% NCBC 800 (engineered biochar from neem chip biochar by 7% $FeCl_3$) was influenced by dosage, pH, temperature, initial concentration, and contact time. The isotherm analysis indicated that the adsorption of methyl orange onto the surface of the engineered biochar is multilayer in nature.

The kinetic models summarized that the adsorption kinetics of engineered biochar, 7% NCBC 800, could be explained clearly by the pseudo-second-order model. The thermodynamic analysis indicated the adsorption of methyl orange onto the engineered biochar surface is endothermic and spontaneous in nature. The adsorptive performance of engineered biochar, 7% NCBC 800, is influenced by boundary layer thickness and inter-particular diffusion rates. The adsorption of organic dye by engineered biochar is influenced by carbon structure and the surface charge distribution as evidenced by XRD and pzc analyses. It is clear from the outcomes of this analysis that the major removal mechanism of methyl orange by engineered biochar is the hydrophobic interaction. The engineered biochar, 7% NCBC 800, exhibited better performance for the removal of color, turbidity, total solids, total suspended solids, and dissolved oxygen of a wastewater sample. Hence, the synthesis of engineered biochar from neem chips, using iron catalyst, is a novel strategy for the effective removal of pollutants from aqueous phase in an efficient manner.

Acknowledgements The authors gratefully acknowledge the support from Department of Agricultural Engineering, Faculty of Agriculture, University of Jaffna, Sri Lanka, to undertake this study. They would also like to thank Department of Civil Engineering, Faculty of Engineering, University of Jaffna, Sri Lanka, for instrumental support. Moreover, they thank Dr. M. Thanihaichelvan, Department of Physics, Faculty of Science, University of Jaffna, Sri Lanka, for the technical support to perform XRD analysis.

Data Availability The datasets generated and/or analyzed during the current study are available from the corresponding author on reasonable request.

Declarations

Conflict of Interest The authors declare no competing interests.

References

Agarwal, A., & Vaishali. (2016). Removal of methyl orange dye from textile effluent using adsorption on chitosan hydrogel beads. *ESSENCE - International Journal for Environmental Rehabilitation and Conservation, VI, I*(2), 73–80.

Ahmed Jasim, M. & Mohammed Abbas, A. (2019). Adsorption of malachite green dye by biomicro-adsorbent from aqueous solution at different temperatures. *Journal of Physics: Conference Series*, *1294*(5). https://doi.org/10.1088/1742-6596/1294/5/052015

Al-wabel, M. I., Al-omran, A., El-naggar, A. H., Nadeem, M., & Usman, A. R. A. (2013). Bioresource technology pyrolysis temperature induced changes in characteristics and chemical composition of biochar produced from Conocarpus wastes. *Bioresource Technology, 131*, 374–379. https://doi.org/10.1016/j.biortech.2012.12.165

Bazrafshan, E., Zarei, A. A., Nadi, H., & Zazouli, M. A. (2014). Adsorptive removal of methyl 827 orange and reactive red 198 dyes by Moringa peregrina ash. *Indian Journal of Chemical Technology, 21*(2), 105–113.

Berwal, N., Kundu, R. S., Nanda, K., Punia, R., & Kishore, N. (2015). Physical, structural and optical characterizations of borate modified bismuth–silicate–tellurite glasses. *Journal of Molecular Structure, 1097*, 37–44.

Bhattacharyya, K. G., & Sharma, A. (2005). Kinetics and thermodynamics of methylene blue adsorption on neem (Azadirachta indica) leaf powder. https://doi.org/10.1016/j.dyepig.2004.06.016

Block, I., Günter, C., Rodrigues, A. D., Paasch, S., Hesemann, P., & Taubert, A. (2021). Carbon adsorbents from spent coffee for removal of methylene blue and methyl orange from water. *Materials*, *14*(14). https://doi.org/10.3390/ma14143996

Bonelli, P. R., Della Rocca, P. A., Cerrella, E. G., & Cukierman, A. L. (2001). Effect of pyrolysis temperature on composition, surface properties and thermal degradation rates of Brazil nut shells. *Bioresource Technology, 76*(1), 15–22. https://doi.org/10.1016/S09608524(00)00085-7

Campos, N. F., Barbosa, C. M. B. M., Rodríguez-Díaz, J. M., & Duarte, M. M. M. B. (2018). Removal of naphthenic acids using activated charcoal: Kinetic and equilibrium studies. *Adsorption Science and Technology, 36*(7–8), 1405–1421. https://doi.org/10.1177/0263617418773844

Chai, W. S., Cheun, J. Y., Kumar, P. S., Mubashir, M., Majeed, Z., Banat, F., Ho, S. H., & Show, P. L. (2021). A review on conventional and novel materials towards heavy metal adsorption in wastewater treatment application. *Journal of Cleaner Production, 296*, 126589. https://doi.org/10.1016/j.jclepro.2021.126589

Farooq, M., & Ramli, A. (2011). The determination of point zero charge (PZC) of Al 2O 3-MgO 847 mixed oxides. *2011 National Postgraduate Conference - Energy and Sustainability: Exploring the Innovative Minds,* NPC 2011, 0–4. https://doi.org/10.1109/NatPC.2011.6136447

Garg, V. K., Gupta, R., Yadav, A. B., & Kumar, R. (2003). Dye removal from aqueous solution by adsorption on treated sawdust. *Bioresource Technology, 89*(2), 121–124. https://doi.org/10.1016/S0960-8524(03)00058-0

Godlewska, P., Bogusz, A., Dobrzyńska, J., Dobrowolski, R., & Oleszczuk, P. (2020). Engineered biochar modified with iron as a new adsorbent for treatment of water contaminated by selenium. *Journal of Saudi Chemical Society, 24*(11), 824–834. https://doi.org/10.1016/j.jscs.2020.07.006

Gökkuş, Ö., & Oğuz, M. (2011). Investigation of color and cod removal by Fenton reagent from aqueous solutions containing acid and reactive dyestuffs. *Desalination and Water Treatment, 26*(1–3), 160–164. https://doi.org/10.5004/dwt.2011.2119

Gökkuş, Ö., Çoşkun, F., Kocaoğlu, M., & Yıldız, Y. Ş. (2014). Determination of optimum conditions for color and COD removal of Reactive Blue 19 by Fenton oxidation process. *Desalination and Water Treatment, 52*(31–33), 6156–6165. https://doi.org/10.1080/19443994.2013.812523

Hamzezadeh, A., Rashtbari, Y., Afshin, S., Morovati, M., & Vosoughi, M. (2022). Application of low-cost material for adsorption of dye from aqueous solution. *International Journal of Environmental Analytical Chemistry, 102*(1), 254–269. https://doi.org/10.1080/03067319.2020.1720011

He, W., Ma, Q., Wang, J., Yu, J., Bao, W., Ma, H., & Amrane, A. (2014). Preparation of novel kaolin-based particle electrodes for treating methyl orange wastewater. *Applied Clay Science, 99*, 178–186. https://doi.org/10.1016/j.clay.2014.06.030

Hii, H. T. (2021). Adsorption isotherm and kinetic models for removal of methyl orang and remazol brilliant blue r by coconut shell activated carbon. *Tropical Aquatic and Soil Pollution, 1*(1), 1–10. https://doi.org/10.53623/tasp.v1i1.4

Iyyapushpam, S., Nishanthi, S. T., & Padiyan, D. P. (2013). Photocatalytic degradation of methyl orange using a -Bi 2 O 3 prepared without surfactant. *Journal of Alloys and Compounds, 563*, 104–107. https://doi.org/10.1016/j.jallcom.2013.02.107

Kloss, S., Zehetner, F., Dellantonio, A., Hamid, R., Ottner, F., Liedtke, V., Schwanninger, M., Gerzabek, M. H., & Soja, G. (2012). Characterization of slow pyrolysis biochars: Effects of feedstocks and pyrolysis temperature on biochar properties. *Journal of Environmental Quality, 41*(4), 990–1000. https://doi.org/10.2134/jeq2011.0070

Kumar, N. S., Shaikh, H. M., Asif, M., & Al-Ghurabi, E. H. (2021). Engineered biochar from wood apple shell waste for high-efficient removal of toxic phenolic compounds in wastewater. *Scientific Reports, 11*(1), 1–17. https://doi.org/10.1038/s41598-021-82277-2

Lonappan, L., Rouissi, T., Brar, S. K., Verma, M., & Surampalli, R. Y. (2018). Adsorption of diclofenac onto different biochar microparticles: Dataset – Characterization and dosage of biochar. *Data in Brief, 16*, 460–465. https://doi.org/10.1016/j.dib.2017.10.041

Manoharan, T., Ganeshalingam, S., & Nadarajah, K. (2022). Mechanisms of emerging contaminants removal by novel neem chip biochar. *Environmental Advances, 7*, 100158. https://doi.org/10.1016/j.envadv.2021.100158

Mohammadi, N., Khani, H., Gupta, V. K., Amereh, E., & Agarwal, S. (2011). Adsorption process of methyl orange dye onto mesoporous carbon material-kinetic and thermodynamic studies. *Journal of Colloid and Interface Science, 362*(2), 457–462. https://doi.org/10.1016/j.jcis.2011.06.067

Nadarajah, K., Bandala, E. R., Zhang, Z., Mundree, S., & Goonetilleke, A. (2021). Removal of 881 heavy metals from water using engineered hydrochar: Kinetics and mechanistic approach. *Journal of Water Process Engineering*, *40*(January), 101929. https://doi.org/10.1016/j.jwpe.2021.101929

Namasivayam, C., & Kavitha, D. (2006). IR, XRD and SEM studies on the mechanism of adsorption of dyes and phenols by coir pith carbon from aqueous phase. *Microchemical Journal, 82*(1), 43–48. https://doi.org/10.1016/j.microc.2005.07.002

Nguyen, L. H., Ngo, Q. N., Van, H. T., Thai, V. N., Nguyen, T. P., & PhanThi, K. O. (2021). Reutilization of Fe-containing tailings ore enriched by iron(III) chloride as a heterogeneous Fenton catalyst for decolorization of organic dyes. *RSC Advances, 11*(26), 15871–15884. https://doi.org/10.1039/d1ra02939h

Pal, J., Deb, M. K., Deshmukh, D. K., & Verma, D. (2013). Removal of methyl orange by activated 892 carbon modified by silver nanoparticles. *Applied Water Science, 3*(2), 367–374. https://doi.org/10.1007/s13201-013-0087-0

Park, H., Kim, J., & Lee, Y. (2021). Enhanced Adsorptive removal of dyes using mandarin peel biochars via Chemical Activation with NH 4 Cl and ZnCl 2.

Sajjadi, B., Chen, W. Y., & Egiebor, N. O. (2019). A comprehensive review on physical activation of biochar for

energy and environmental applications. *Reviews in Chemical Engineering, 35*(6), 735–776. https://doi.org/10.1515/revce-2017-0113

Samar K. Theydan, M. J. A. (n.d.). Adsorption of methylene blue onto biomass-based activated carbon by FeCl3 activation: Equilibrium, kinetics, and thermodynamic studies. *Journal of Analytical and Applied Pyrolysis*. https://doi.org/10.1016/j.jaap.2012.05.008

Soldatkina, L., & Zavrichko, M. (2019). Equilibrium, kinetic, and thermodynamic studies of anionic dyes adsorption on corn stalks modified by cetylpyridinium bromide. *Colloids and Interfaces*, *3*(1). https://doi.org/10.3390/colloids3010004

Song, M., Jin, B., Xiao, R., Yang, L., Wu, Y., Zhong, Z., & Huang, Y. (2013). The comparison of two activation techniques to prepare activated carbon from corn cob. *Biomass and Bioenergy, 48*, 250–256. https://doi.org/10.1016/j.biombioe.2012.11.007

Soylu, M., Gökkuş, Ö., & Özyonar, F. (2020). Foam separation for effective removal of disperse and reactive dyes from aqueous solutions. *Separation and Purification Technology*, *247*(December 2019). https://doi.org/10.1016/j.seppur.2020.116985

Wasewar, K. L., Prasad, B., & Gulipalli, S. (2009). Removal of selenium by adsorption onto granular activated carbon (GAC) and powdered activated carbon (PAC). *Clean - Soil, Air, Water, 37*(11), 872–883. https://doi.org/10.1002/clen.200900188

Yönten, V., Sanyürek, N. K., & Kivanç, M. R. (2020). A thermodynamic and kinetic approach to adsorption of methyl orange from aqueous solution using a low cost activated carbon prepared from Vitis vinifera L. *Surfaces and Interfaces, 20*, 100529. https://doi.org/10.1016/j.surfin.2020.100529

Zhang, Z., Moghaddam, L., O'Hara, I. M., & Doherty, W. O. S. (2011). Congo Red adsorption by ball-milled sugarcane bagasse. *Chemical Engineering Journal, 178*, 122–128. https://doi.org/10.1016/j.cej.2011.10.024

Zhu, C., Wang, L., Kong, L., Yang, X., Wang, L., Zheng, S., Chen, F., Maizhi, F., & Zong, H. (2000). Photocatalytic degradation of AZO dyes by supported TiO22 + UV in aqueous solution. *Chemosphere, 41*(3), 303–309. https://doi.org/10.1016/S0045-6535(99)00487-7